BIOCHEMISTRY
including biophysical chemistry & molecular biology

Article

pubs.acs.org/biochemistry

Staphylococcus aureus CstB Is a Novel Multidomain Persulfide Dioxygenase-Sulfurtransferase Involved in Hydrogen Sulfide Detoxification

Jiangchuan Shen,[†,‡] Mary E. Keithly,[§] Richard N. Armstrong,[§,∥,⊥] Khadine A. Higgins,[†,#] Katherine A. Edmonds,[†] and David P. Giedroc*[,†,‡]

[†]Department of Chemistry, [‡]Graduate Program in Biochemistry, Indiana University, Bloomington, Indiana 47405, United States
[§]Department of Chemistry, Vanderbilt University, Nashville, Tennessee 37232, United States
[∥]Department of Biochemistry, Vanderbilt University School of Medicine, Nashville, Tennessee 37232-6304, United States

Supporting Information

ABSTRACT: Hydrogen sulfide (H_2S) is both a lethal gas and an emerging gasotransmitter in humans, suggesting that the cellular H_2S level must be tightly regulated. CstB is encoded by the *cst* operon of the major human pathogen *Staphylococcus aureus* and is under the transcriptional control of the persulfide sensor CstR and H_2S. Here, we show that CstB is a multifunctional Fe(II)-containing persulfide dioxygenase (PDO), analogous to the vertebrate protein ETHE1 (ethylmalonic encephalopathy protein 1). Chromosomal deletion of *ethe1* is fatal in vertebrates. In the presence of molecular oxygen (O_2), hETHE1 oxidizes glutathione persulfide (GSSH) to generate sulfite and reduced glutathione. In contrast, CstB oxidizes major cellular low molecular weight (LMW) persulfide substrates from *S. aureus*, coenzyme A persulfide (CoASSH) and bacillithiol persulfide (BSSH), directly to generate thiosulfate (TS) and reduced thiols, thereby avoiding the cellular toxicity of sulfite. Both Cys201 in the N-terminal PDO domain ($CstB^{PDO}$) and Cys408 in the C-terminal rhodanese domain ($CstB^{Rhod}$) strongly enhance the TS generating activity of CstB. CstB also possesses persulfide transferase (PT; reverse rhodanese) activity, which generates TS when provided with LMW persulfides and sulfite, as well as conventional thiosulfate transferase (TST; rhodanese) activity; both of these activities require Cys408. CstB protects *S. aureus* against H_2S toxicity, with the C201S and C408S *cstB* genes being unable to rescue a NaHS-induced Δ*cstB* growth phenotype. Induction of the *cst* operon by NaHS reveals that functional CstB impacts cellular TS concentrations. These data collectively suggest that CstB may have evolved to facilitate the clearance of LMW persulfides that occur upon elevation of the level of cellular H_2S and hence may have an impact on bacterial viability under H_2S misregulation, in concert with the other enzymes encoded by the *cst* operon.

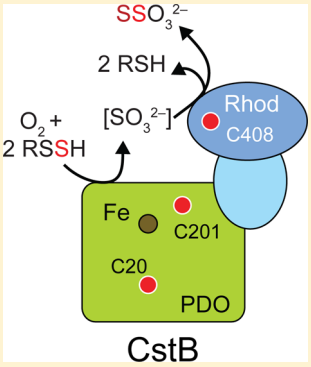

Hydrogen sulfide (H_2S) is a colorless and flammable gas that has a strong rotten egg smell and can freely pass through biological membranes. In the cell, it primarily exists as hydrosulfide anion (HS^-).[1] H_2S inhibits cellular respiration by poisoning the terminal electron acceptor cytochrome c oxidase at submicromolar concentrations.[2−4] H_2S may also exhibit toxicity when HS^- reacts directly with the oxidized low molecular weight (LMW) thiols that collectively control the cellular redox potential, e.g., glutathione disulfide (GSSG) or bacillithiol disulfide (BSSB), to form reactive sulfur species (RSS),[5] glutathione or bacillithiol persulfides (GSSH, BSSH).[6] Recent studies reveal that H_2S can also play positive biological roles. In mammalian systems, H_2S has been characterized as a gasotransmitter or signaling molecule that influences a number of processes, including vasorelaxation, cardioprotection, and neurotransmission.[7−9] In many bacteria, endogenous production of H_2S by three major H_2S-generating enzymes, cystathionine *β*-synthase (CBS), cystathionine *γ*-lyase (CSE), and 3-mercaptopyruvate sulfur transferase (3-MST), has been shown to enhance resistance to oxidative stress induced by antibiotic treatment via an unknown mechanism.[10]

This combination of toxicity and utility of H_2S suggests a physiological need to regulate intracellular H_2S concentrations. One example of such regulation in eukaryotic systems is the mitochondrial persulfide dioxygenase (PDO), ethylmalonic encephalopathy protein 1 (ETHE1). Chromosomal deletion of *ethe1* causes ethylmalonic encephalopathy and is ultimately fatal, due to H_2S toxicity.[11] Although there is a report of a HS^- efflux transporter from the human pathogen *Clostridium difficile*,[12] major H_2S detoxification mechanisms in bacteria remain poorly understood.

Staphylococcus aureus is a Gram-positive opportunistic pathogen that causes a wide variety of hospital- and community-acquired infections, ranging from minor skin infections to life-threatening diseases[13] With no gene encoding 3-MST, *S. aureus* relies on CBS and CSE for the synthesis of endogenous H_2S.[10] We recently described the *cst* (copper-sensing operon repressor-like sulfur transferase) operon,[14]

Received: May 29, 2015
Revised: July 2, 2015
Published: July 6, 2015

DOI: 10.1021/acs.biochem.5b00584
Biochemistry 2015, 54, 4542−4554

which appears to be crucial for sulfide detoxification in *S. aureus* (Figure 1). Transcription of the *cst* operon is regulated by a

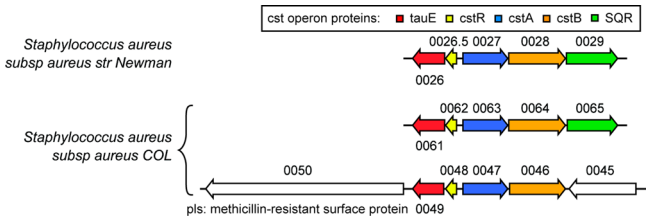

Figure 1. Genomic region of *S. aureus* subspecies aureus strains Newman (top) and COL (middle, bottom) encompassing the *cst* operon region. Locus tag identifiers are indicated as NWMN_0029–NWMN_0026 (top) encoding SQR (shaded green), CstB (orange), CstA (blue), CstR (yellow), and TauE (red), SACOL0065–SACOL0061 (middle), and duplicated in the strain COL as SACOL0045–SACOL0050 (bottom), shaded as indicated for the Newman strain. The duplicated core *cst* operon region (SACOL0046–SACOL0049; *cstB2*, *cstA2*, *cstR2*, *tauE2*) is upstream of a methicillin-resistance determinant (SACOL0050, *pls* or methicillin-resistance surface protein) and downstream of the *mecA*, *mecR1*, and *mecI* genes (not shown), encoding the penicillin binding protein 2A, a β-lactam sensor/signal transducer membrane protein that binds methicillin, and the methicillin-resistance repressor, respectively (Figure S1). CstB encoded by NWMN_0028 is the subject of the studies reported here.

per- and polysulfide-sensing repressor, CstR, and is induced upon addition of exogenous NaHS or polysulfides to cells grown aerobically in liquid culture.[15] Three of the genes encoded by the *cst* operon, including *cstA*, *cstB*, and *sqr*, the latter encoding a sulfide:quinone oxidoreductase, are necessary to mitigate the effects of cellular sulfide toxicity.[15] The core *cst*-encoded genes, *tauE*, *cstR*, *cstA*, and *cstB*, are often duplicated in methicillin-resistant strains of *S. aureus* (MRSA), and a synteny analysis reveals that this copy is flanked by methicillin-resistance determinants from the major staphylococcal cassette chromosome *mec* element types (SCCmec) (Figure S1).

CstA has recently been characterized as a multidomain sulfurtransferase that reacts with a persulfide formed on the cysteine desulfurase SufS as well as with inorganic polysulfides such as sodium tetrasulfide.[16] SQR and CstB, on the other hand, are predicted to comprise a system analogous to the first two steps in human mitochondrial H_2S oxidation. Human SQR (hSQR) initially oxidizes H_2S to glutathione persulfide (GSSH); subsequently, ETHE1 oxidizes GSSH to sulfite in the presence of molecular oxygen while regenerating reduced glutathione (GSH).[17] In the mitochondrion, toxic sulfite[18] can be further oxidized to thiosulfate (TS) via a persulfide transferase (PT; also known as a reverse rhodanese) activity or to sulfate via the molybdopterin-requiring enzyme sulfite oxidase. Since *S. aureus* encodes no known sulfite oxidase, we surmise that sulfite is either assimilated by one of four identified cellular rhodaneses including those found in CstA and CstB[19] or is effluxed from the cell via an unknown mechanism.[20]

CstB is predicted to be a three-domain enzyme containing an N-terminal metallo-β-lactamase-like (MBL), a nonheme Fe(II)-containing PDO domain, followed by a pseudorhodanese homology (RHD) domain, and a conventional C-terminal rhodanese (Rhod) domain (Figure 2A). The N-terminal PDO domain of CstB is homologous to full-length human ETHE1, with 21% identity (Figure S2), as well as to *Arabidopsis* ETHE1.[21,22] The conserved iron-binding residues in the active site (Figure S2) are highlighted in the crystal structure of hETHE1 shown in the left panel of Figure 2B.[23] Although this enzyme forms the basis for our hypotheses regarding the enzymatic activity of CstB, such relatively low sequence identity leads us to anticipate important structural differences that impact enzyme function.

A number of structural genomics initiatives have provided several crystal structures that collectively provide additional perspectives on CstB function. These structures include CstB2 from *S. aureus* strain COL, which shows the N-terminal PDO and middle RHD domains but lacks the C-terminal Rhod domain (Figure 2B, middle panel). This protein is 77% identical to CstB from *S. aureus* strain Newman and is representative of CstBs contained within a duplicated core *cst* operon in the COL (SACOL0046; Figure 1) and other methicillin-resistant *S. aureus* strains (Figure S1); SACOL0064-encoding CstB1 is 100% identical to the Newman-strain CstB studied here (Figure 1). The structure of the CstB2 PDO domain is similar to that of hETHE1 and that of ETHE1 from *Arabidopsis thaliana*,[21,22] except for the presence a long, cysteine-containing loop near the iron active site, highlighted in Figure 2B. Like ETHE1, the CstB2 structure also shows Fe(II) bound in a semifacial triad composed of the side chains of H56, H119, and D145 (Figure 2B, inset). Another related structure comes from an *Alicyclobacillus acidocaldarius* protein with a very similar domain organization as that of full-length CstB (3TP9$^{\text{PDO-RHD-Rhod}}$) (Figure 2B, right panel). This protein is 52% identical to CstB and contains all three cysteine residues that are conserved in *S. aureus* CstB (equivalent to C20, C201, and C408, highlighted in Figures 2B and S1). The N-terminal and middle domains are oriented similarly to the CstB2 structure, suggesting that the three domains of CstB might pack together in a similar orientation in order to function collaboratively.

In this work, we show that CstB catalyzes the oxidation of major LMW persulfides from *S. aureus*, coenzyme A persulfide (CoASSH) and bacillithiol persulfide (BSSH) and to a lesser extent cysteine persulfide (CSSH) and glutathione persulfide (GSSH), to TS and reduced thiols, in contrast to the sulfite-generating activity of ETHE1.[17] CstB is also shown to be a multifunctional enzyme that harbors persulfide transferase (PT) and conventional thiosulfate transferase (TST) activities, both catalyzed by the CstB$^{\text{Rhod}}$ domain. All three cysteine residues of CstB, C20, C201, and C408, are crucial for cellular viability under NaHS stress despite the fact that C20 and C201 are not conserved in eukaryotic PDOs. This work represents the first characterization of a multidomain bacterial PDO-RHD-Rhod fold protein from a human pathogen, and the potential significance of these findings on *S. aureus* physiology is discussed, in concert with the other known activities of *cst*-encoded gene products.[15,16]

MATERIALS AND METHODS

Cloning and Purification of Recombinant CstB Proteins. Full-length CstBs (wild-type, C20S, C201S, C408S, and C201S/C408S) and CstB$^{\text{PDO-RHD}}$ were cloned into a pET15b expression plasmid using the *Nco*I and *Bam*HI restriction sites. CstB$^{\text{Rhod}}$ was cloned into pHis parallel expression plasmid using *Nco*I and *Sal*I restriction sites. CstB mutants (C20S, C201S, and C408S) were generated by site-directed mutagenesis. All CstB expression plasmids were transformed into the *E. coli Rosetta* strain, cultured in LB medium at 37 °C until the OD_{600} reached 0.6–0.8, induced

DOI: 10.1021/acs.biochem.5b00584
Biochemistry 2015, 54, 4542–4554

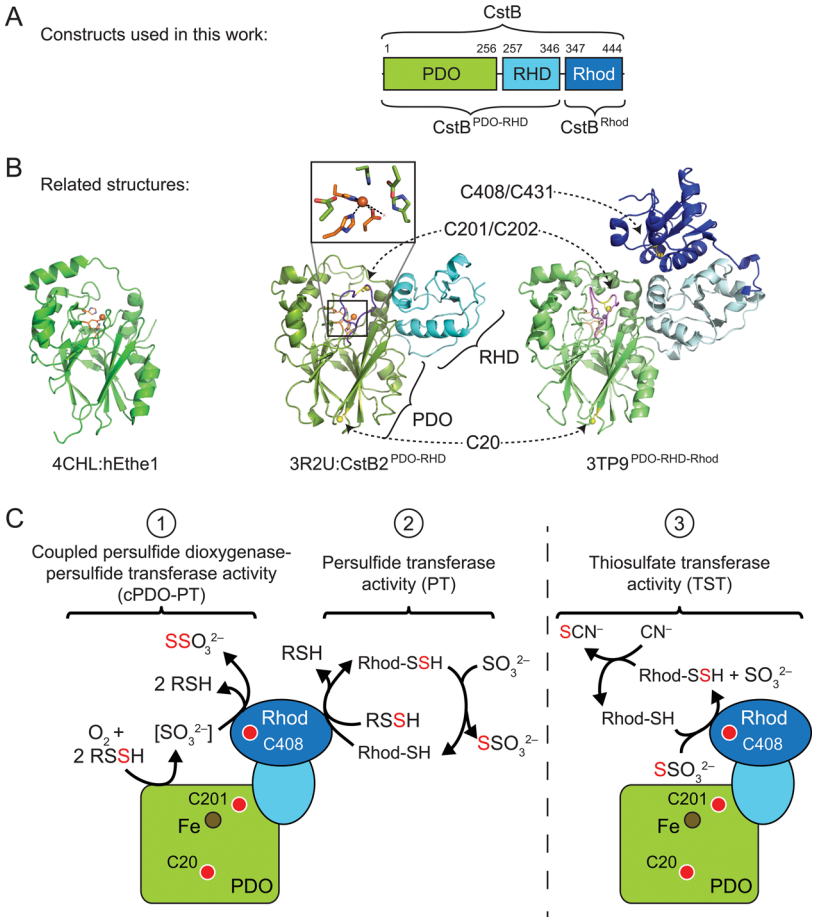

Figure 2. Structural overview of CstB and related enzymes. (A) Domain organization of *S. aureus* CstB, with N-terminal persulfide dioxygenase (PDO) domain, middle rhodanese homology domain (RHD), and C-terminal rhodanese domain (Rhod). (B) Structures of CstB homologues previously published or from structural genomics efforts: hETHE1 (PDB 4CHL, left panel), *S. aureus* COL CstB2$^{PDO-RHD}$ (PDB 3R2U, middle panel), and *A. acidocaldarius* homologue of unknown function (PDB 3TP9, right panel). PDO domains are shaded green, RHD, light blue, and rhodanese domains, dark blue. Conserved metal-binding side chain ligands are highlighted in orange, and conserved cysteines, yellow. The extended loop containing C201 that is not present in hETHE1 is highlighted in purple in the other two structures. (C) Cartoon model of *S. aureus* CstB highlighting the three catalytic activities documented here: coupled persulfide dioxygenase-persulfide transferase (cPDO-PT) activity, reaction 1; persulfide transferase (PT) activity, reaction 2; and rhodanese or thiosulfate transferase (TST) activity, reaction 3. Approximate locations of conserved cysteines and Fe center are indicated by the red and brown circles, respectively. In all panels, the PDO domain is shaded green, RHD, light blue, and Rhod, domain dark blue.

with 1 mM IPTG, and expressed at 16 °C for 16 h. Cells were harvested by centrifugation and stored at −80 °C.

Full-length CstBs (wild-type, C201S, C408S, and C201S/C408S) and CstB$^{PDO-RHD}$ were all purified using similar protocols. The cell pellet was resuspended in 25 mM HEPES, 150 mM NaCl, 5 mM DTT, 2 mM EDTA, pH 7.0, and lysed by sonication. The cell lysate was clarified by centrifugation, and 0.015% (w/v) polyethylenimine (PEI) was added to the supernatant to precipitate nucleic acids and nucleic acid binding proteins. Full-length CstBs coprecipitated with nucleic acids with the addition of 0.015% (w/v) PEI and were redissolved by stirring the pellet in 25 mM Tris-HCl, 1 M NaCl, 5 mM DTT, 2 mM EDTA, pH 8.0, for 2 h at 4 °C. Ammonium sulfate (AS) precipitation was next performed to salt out full-length CstBs between 40 and 60% (w/v) AS. CstB$^{PDO-RHD}$ remained in solution with the addition of 0.015% (w/v) PEI and was salted out between 30 and 50% (w/v) AS directly. Ammonium sulfate pellets were then resuspended in 25 mM Tris-HCl, 50 mM NaCl, 5 mM DTT, 2 mM EDTA, pH 8.0, and CstB proteins were purified by anion exchange chromatography (Q-sepharose) followed by size exclusion chromatography (G200 16/60). Fractions containing target proteins with a purity of >95%, as evaluated by SDS-PAGE analysis, were pooled and stored at −80 °C until use with 20% (v/v) final concentration of glycerol added.

CstB^{Rhod} was purified by Ni-NTA affinity chromatography followed by removal of the N-terminal His_6-tag. The cell pellet was resuspended in 25 mM Tris-HCl, 500 mM NaCl, 20 mM imidazole, 2 mM TCEP, pH 8.0, and lysed by sonication. The cell lysate was clarified by centrifugation, and the supernatant was loaded on a Ni-NTA column, which was pre-equilibrated with lysis buffer. The column was washed with lysis buffer containing 50 mM imidazole, followed by elution with 500 mM imidazole. His_6-CstB^{Rhod} was exchanged into lysis buffer and incubated with tobacco etch virus (TEV) protease at 4 °C overnight. The cleaved His_6 tag was removed by reapplication of the TEV-incubated protein to the Ni-NTA column, and the cleaved CstB^{Rhod} was collected in the flow-through and in the 50 mM imidazole wash fractions, followed by further purification by size exclusion chromatography (G75 16/60). Fractions containing CstB^{Rhod} with a purity of >95% were

DOI: 10.1021/acs.biochem.5b00584
Biochemistry 2015, 54, 4542−4554

pooled and stored at −80 °C until use with 20% (v/v) final concentration of glycerol added.

Metal Analysis. Wild-type CstB was analyzed by inductively coupled plasma mass spectrometry (ICP-MS) to confirm that iron (Fe) was the only significant metal found, with undetectable zinc (Zn), cobalt (Co), manganese (Mn), and nickel (Ni). The Fe content for all CstBs was then quantified by atomic absorption spectroscopy (AAS), utilizing proteins prepared at 20 μM in 25 mM Tris-HBr, 100 mM NaBr, pH 8.0, as follows: all CstBs were exchanged into degassed and chelexed, metal-free 25 mM Tris-HBr, 100 mM NaBr, pH 8.0, in an anaerobic chamber to remove reducing reagents and EDTA, then loaded with Fe by exchanging into 25 mM Tris-HBr, 100 mM NaBr, 10 mM $FeSO_4$, 10 mM $Na_2S_2O_4$, pH 8.0, and finally into 25 mM Tris-HBr, 100 mM NaBr, pH 8.0, to remove free Fe.

EPR Spectroscopy. X-band EPR spectroscopy was carried out in the NMR Facility, Department of Chemistry, essentially as described[24] and was used to estimate the total Fe(III) content in wild-type CstB following anaerobic loading of Fe to a stoichiometry of 1:1 and subsequent reduction with sodium dithionite.[17] Fe(III) was quantified by comparison to a series of standard solutions acquired under the same conditions. 200 μM Fe(II)-loaded CstB was found to contain 18 μM Fe(III), revealing ≈90% Fe(II) in this preparation. Multiple preparations of CstB contained similar specific activities. All other mutant CstB preparations were assumed to harbor largely reduced Fe(II) as a result of this anaerobic reconstitution procedure.

Gel Filtration Chromatography. All CstBs containing stoichiometric Fe were chromatographed on an analytical G200 GL column by loading 100 μL at 10 μM protomer concentration protein and eluting at 0.5 mL/min at 4 °C. $CstB^{Rhod}$ was chromatographed on an analytical G75 column by loading 100 μL of 20 μM protomer concentration protein and eluting at 0.5 mL/min at 4 °C.

Preparation of LMW Persulfide Substrates. Bacillithiol disulfide (BSSB) was synthesized by the Vanderbilt Chemical Synthesis Core and reduced to BSH according to published procedures.[25] All other reduced thiols and disulfides were obtained from commercial sources and used without further purification. LMW persulfides were freshly prepared by mixing a 5-fold molar excess of sodium sulfide (Na_2S) with oxidized LMW disulfide and incubating anaerobically at 30 °C for 30 min in degassed 300 mM phosphate, pH 7.4. The concentration of generated LMW persulfides was determined using a cold cyanolysis assay and used without further purification in enzymatic assays at the indicated final concentration.[17]

Coupled Persulfide Dioxygenase-Persulfide Transferase (cPDO-PT) Activity Assays. The cPDO-PT activity was measured using a fluorescence-based HPLC assay to detect the production of TS as outlined previously.[15] Typical 100 μL reactions contained 40 nM CstBs and a specific LMW persulfide substrate ranging from 40 μM to 2.56 mM, buffered by air-saturated 25 mM MES, 100 mM NaBr, pH 6.0, at 25 °C. These reactions were initiated with the addition of enzyme or BSA (as a control), incubated for 2 min, and terminated by addition of 0.5 μL of 5 M methanesulfonic acid (MA). Proteins were removed by ultrafiltration, and 25 μL of the filtered solution was labeled in the dark by 75 μL of monobromobimane (mBBr) labeling solution containing 25 mM Tris-HBr, 2 M mBBr, pH 8.0, for 30 min at room temperature. The labeling reaction was terminated by addition of 100 μL of 16.4% methanol, 0.25% acetic acid, pH 3.9. Twenty microliter samples were injected in duplicate onto a Kinetex C18 reversed-phase column (Phenomenex, no. 00F-4601-E0, 4.6 mm × 150 mm, 5 μm, 100 Å) outfitted with a Zorbax Eclipse Plus C18 guard column, followed by chromatographic analysis on a Waters 600 high-performance liquid chromatography system equipped with a Waters 717 plus autosampler, a Waters 474 scanning fluorescence detector (λ_{ex} = 384 nm and λ_{em} = 478 nm), and Empower chromatography software installed on a standard PC running Windows XP. A methanol-based gradient system was employed to analyze the samples at 25 °C (solvent A: 16.8% methanol, 0.25% acetic acid, pH 3.9; solvent B: 90% methanol, 0.25% acetic acid, pH 3.9) with a flow rate of 1.2 mL/min and an elution protocol as follows: 0−10 min, 0% B isocratic; 10−12 min, 0−100% B, linear gradient; 12−17 min, 100% B isocratic followed by re-equilibration to 0% B. Quantitation of TS was enabled by running a series of authentic TS standards in separate chromatographic runs with an identical protocol. For time course studies, 200 μL reactions containing 10 μM CstB and 200 μM persulfide substrate in 25 mM MES, 100 mM NaBr, pH 6.0, at 25 °C were used. Here, the reactions were initiated as above and terminated at various times, from 0 to 32 min, by adding 1 μL of 5 M methanesulfonic acid (MA). Fifty microliters of the ultrafiltered solution was labeled in the dark by 50 μL of mBBr labeling solution containing 25 mM Tris-HBr, 2 M mBBr, pH 8.0, for 30 min at room temperature. The labeling reaction was terminated by addition of 100 μL of 16.8% methanol, 0.25% acetic acid, pH 3.9, and 40 μL samples were subjected to chromatographic analysis as described above.

Persulfide Transferase (PT) Activity Assays. The PT activity was measured using the fluorescence-based HPLC assay described above for TS production. Five-hundred microliter reactions contained 200 nM C201S CstB or $CstB^{2CS}$ or BSA (as a control) and a specific persulfide substrate ranging from 8 to 384 μM and 200 μM sulfite buffered in degassed 25 mM MES, 100 mM NaBr, pH 6.0, at 25 °C. The reaction was initiated in the anaerobic chamber by sulfite, incubated for 2 min, and terminated by addition of 2.5 μL of 5 M MA. Fifty microliters of the ultrafiltered solution was labeled in the dark with 50 μL of mBBr labeling solution containing 25 mM Tris-HBr, 2 M mBBr, pH 8.0, for 30 min at room temperature. These reactions were analyzed as described above for the cPDO-PT activity assays.

Thiosulfate Transferase (TST) Activity Assays. Purified CstBs were preincubated with 1000-fold molar excess of potassium cyanide (KCN) (prepared as 2 M KCN stock in 100 mM Tris-HCl, pH 8.0) at room temperature for 1 h to strip any persulfide sulfur on the cysteine residues that may have occurred during purification. KCN-treated CstBs were then extensively exchanged into fully degassed 25 mM Tris-HBr, 100 mM NaBr, pH 8.0, in an anaerobic chamber to remove KCN. The TST activity was measured using a cold cyanolysis assay for the thiocyanate production essentially as described previously for CstA proteins.[16] One milliliter reactions contained 400 nM CstBs, 50 mM KCN, and TS ranging from 100 μM to 6.4 mM, buffered by 100 mM MES, pH 6.0, at 37 °C, with the reactions initiated with the addition of enzyme, incubated for 4 min, and terminated by addition of 2 mL of Fe/formaldehyde solution [50 g/L $Fe(NO_3)_3$ in 65% HNO_3/37% formaldehyde = 1:3 (v/v)]. The potassium thiocyanate (KSCN) production was measured using a 96-well plate reader for absorption at 460 nm for the generated thiocyanato iron

DOI: 10.1021/acs.biochem.5b00584
Biochemistry 2015, 54, 4542−4554

Table 1. Molecular Weights and Iron Binding Stoichiometries of Wild-Type and Mutant CstBs

protein	molecular mass (Da)[a]	molecular mass (Da)[b] (calculated)	molecular mass (Da) gel filtration[c]	Fe content as purified (mol Fe/mol protomer)	Fe content post loading (mol Fe/mol protomer)
CstB	49 275.8	49 277.4	220 000	0.5 ± 0.1	1.0 ± 0.1
C201S CstB	49 262.5	49 261.3	221 000	0.5 ± 0.1	1.0 ± 0.1
C408S CstB	49 262.3	49 261.3	298 000	0.5 ± 0.1	1.0 ± 0.1
$CstB^{2CS}$	49 243.9	49 245.2	293 000	0.5 ± 0.1	1.0 ± 0.1
$CstB^{PDO-RHD}$	38 333.2	38 334.3	147 000	0.3 ± 0.2	1.0 ± 0.1
$CstB^{Rhod}$	11 132.9	11 133.3	34 000	N/A	N/A

[a]Protomer molecular mass measured by ESI MS. [b]Calculated from the amino acid sequence. [c]Native chromatography on Sepharose G200 GL, 10–20 μM protomer, pH 8.0.

complex. Quantitation of KSCN was enabled by running a series of authentic KSCN standards in separate runs using an identical protocol.

Cell Growth. *S. aureus* Newman strains were inoculated from glycerol stocks and grown in 5 mL of tryptic soy broth (TSB) medium with 10 μg/mL chloramphenicol overnight, as all the strains carry either the empty pOS1 vector (wild-type strain and Δ*cstB* strain) or the indicated *cstB* alleles constructed in the pOS1 vector.[15] The overnight cultures were pelleted by centrifugation, resuspended in equal volume of Hussain–Hastings–White modified (HHWm) medium, and diluted into 15 mL of HHWm supplemented with 0.5 mM TS, in the presence and absence of 0.2 mM NaHS. All cultures (≈25 mL) were grown aerobically at 37 °C in duplicate with shaking at 200 rpm in loosely capped 50 mL Falcon tubes. Cell density was recorded hourly for 10 h by removal of 0.5 mL and measurement of optical density at 600 nm. The starting OD_{600} of each culture was ≈0.008.

Measurement of Cellular TS Concentration. All *S. aureus* wild-type, Δ*cstB*, and complemented strains were grown in 10 mL of TSB medium with 10 μg/mL chloramphenicol overnight. Cells were pelleted and washed with phosphate buffered saline (PBS), and cultures were initiated at OD_{600} of ≈0.02 in HHWm medium with 10 μg/mL chloramphenicol and 0.5 mM TS as the sole sulfur source. NaHS was added to the cultures at a final concentration of 0.2 mM when the OD_{600} reached ≈0.2. All cultures were grown in loosely capped 50 mL Falcon tubes at 37 °C with shaking at 200 rpm. Aliquots were removed at 0, 10, 30, 60, and 120 min following addition of NaHS (equivalent to 15 mL of OD_{600} = 0.2 cells) and harvested by centrifugation at 3000 rpm for 10 min, with the culture medium supernatant being discarded. Cell pellets were then washed with PBS, pelleted again by centrifugation at 13 200 rpm for 5 min, and stored frozen at −80 °C until analysis. Cell pellets were then thawed, resuspended in 100 μL of mBBr labeling solution containing 20 mM Tris-HBr, pH 8.0, 50% acetonitrile, 1 mM mBBr, and 2 μM *N*-acetyl-L-cysteine (NAC) for use as an internal standard, and incubated at 60 °C for 1 h in the dark in screw capped Eppendorf tubes to avoid liquid loss by evaporation. Cellular debris and proteins were then pelleted by centrifugation at 13 200 rpm for 5 min, and the supernatant was transferred to a fresh Eppendorf tube containing 300 μL of 10 mM MA to terminate the labeling reaction. These samples were centrifuged at 13 200 rpm for 5 min through 0.2 μm centrifugal filter unit to remove particulates, and 40 μL samples were injected onto a Kinetex C18 reversed-phase column exactly as described above. Duplicate samples were typically analyzed using the a methanol-based gradient system (solvent A: 10% methanol, 0.25% acetic acid, pH 3.9; solvent B: 90% methanol, 0.25% acetic acid, pH 3.9) with the elution protocol at 25 °C and a flow rate of 1.2 mL/min as follows: 0–10 min, 0% B isocratic; 10–22 min, 0–24% B, linear gradient; 24–32 min, 24% B isocratic; 32–45 min, 24–45% B, linear gradient; 45–50 min, 45–82% B, linear gradient; 50–52 min, 82–100% B, linear gradient, followed by re-equilibration to 0% B. Quantitation of TS was enabled by running a series of authentic TS standards in separate chromatographic runs with the identical protocol.

RESULTS

Purification and Biochemical Characterization of CstB and CstB Mutants, $CstB^{PDO-RHD}$ and $CstB^{Rhod}$. Intact wild-type and CstB mutants (C201S and C408S) were purified to >95% purity, with molecular masses confirmed by ESI mass spectrometry (Table 1). All enzymes contained the full complement of reduced cysteines, as determined by a DTNB assay.[26] Because crystal structures show that both ETHE1 and the *S. aureus* COL CstB2 bind Fe(II) in a semifacial triad of protein-derived ligands (Figure 2B), we predicted that the side chains of H56, H119, and D145 coordinate Fe(II) in CstB. Indeed, purified CstBs contain ∼0.5 mol equivalent of iron per protomer as isolated, and each is capable of binding iron up to a ratio of 1:1 upon anaerobic addition of excess exogenous Fe(II), followed by separation of bound from free Fe(II) (Table 1). EPR studies of purified CstB show that the oxidation state is ≥90% Fe(II) following anaerobic reduction with dithionite.

Analytical gel filtration experiments show that Fe(II)-loaded wild-type CstB is tetrameric (226 kDa), as is C201S CstB and the truncated $CstB^{PDO-RHD}$ (Table 1 and Figure S4A,B). These findings are in contrast to hETHE1, which exists in a monomer–dimer equilibrium in solution,[23] but they are consistent with the D_2-symmetric assembly state observed in the crystal structure of CstB2 (Figure S3). This structure shows the middle RHD domain mediates most of the intersubunit contacts in the solid state; CstB from *S. aureus* strain Newman likely adopts a similar architecture in solution. In contrast, chromatography of C408S CstB results in a smaller retention time and larger apparent molecular weight, ≈298 kDa (Table 1 and Figure S4C). The same apparent molecular weight is obtained for the double C201S/C408S CstB, designated $CstB^{2CS}$ (Table 1 and Figure S4D). This suggests that C408S CstB and $CstB^{2CS}$ each exist as hexamers or, alternatively, more poorly packed and hydrodynamically larger tetramers, perhaps harboring a destabilized C-terminal Rhod domain. A homonuclear $^1H-^1H$ NOESY spectrum of the isolated $CstB^{Rhod}$ (residues 347–444) shows mostly broad lines and a few very sharp resonances found in the random-coil region of the amide spectrum (Figure S5); this isolated domain also results in an oligomeric, mostly trimeric, assembly state (Table

DOI: 10.1021/acs.biochem.5b00584
Biochemistry 2015, 54, 4542–4554

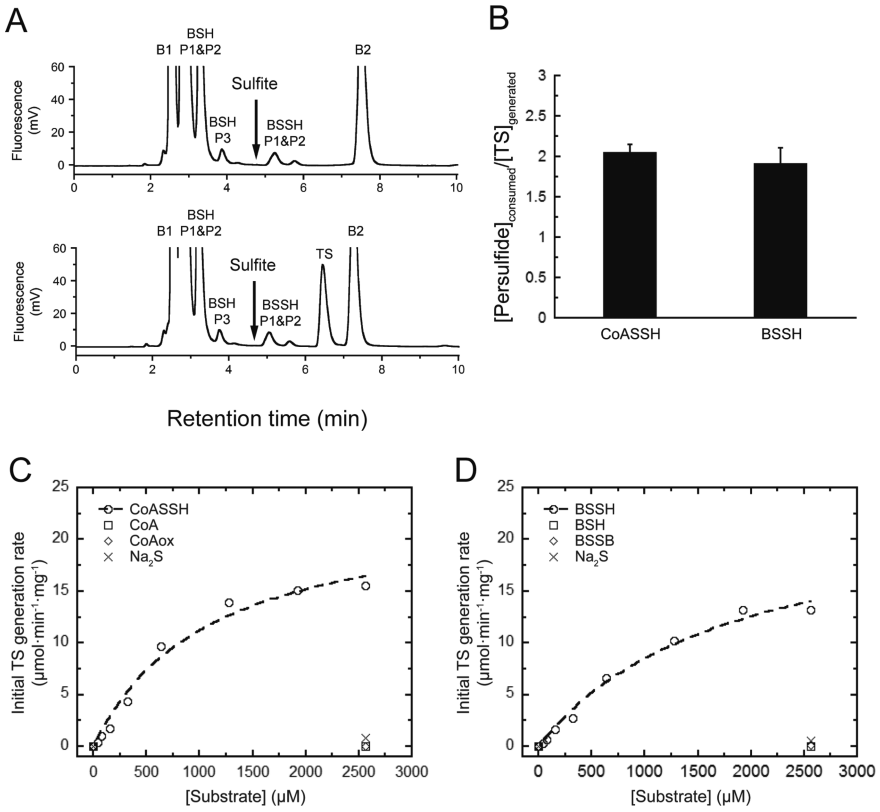

Figure 3. Coupled persulfide dioxygenase-persulfide transferase (cPDO-PT) activity of CstB with various persulfide substrates. (A) Representative LC-based assays used to measure reactant−product profiles of cPDO-PT activity with BSSH at t = 0 min (top trace) and t = 2 min (bottom trace) as substrates at 400 nM CstB. The chromatographic position of sulfite is indicated by the arrow.[15] Note that B1 and B2 peaks are from labeling buffer; labeled BSH displays as two major peaks (BSH P1 and P2) and one minor peak; BSSH is highly unstable in the aerobic buffer used here to lyse the cells and thus is underestimated as two small peaks (BSSH P1 and P2). The concentration was alternatively measured using a cold cyanolysis assay.[17] (B) Stoichiometry of persulfide substrates consumed (CoASSH and BSSH) versus TS generated for cPDO-PT activity of CstB. The molar ratio of CoASSH consumed to TS generated is ≈1.9, and that of BSSH consumed to TS generated is ≈2.1 in in multiple experiments carried out at 400 nM CstB. (C) Initial TS generation rates as a function of concentrations of CoASSH (open circles) vs CoA (open squares), CoA^{ox} (open diamonds), and Na_2S (crosses). The dashed, continuous line through the open circles is a fit to the Michaelis−Menten equation, with parameters summarized in Table 2. (D) Initial TS generation rates as a function of the concentrations of BSSH (open circles) vs BSH (open squares), BSSB (open diamonds), and Na_2S (crosses). The dashed, continuous line through the open circles is a fit to the Michaelis−Menten equation, with parameters summarized in Table 2.

1 and Figure S4F). These data suggest that C-terminal Rhod domain may be poorly folded in the absence of the rest of CstB, consistent with the considerable interdomain packing shown in the structure of the *A. acidocaldarius* CstB-like protein (Figure 2B, right panel). Likewise, substitution of the presumed Rhod active-site C408 also appears to destabilize the native fold. Efforts to purify a core ETHE1-like $CstB^{PDO}$ domain (residues 1−256) were also unsuccessful due to insolubility in bacterial lysates, rationalized by the appreciable packing of the N-terminal PDO and middle RHD domains (Figure 2B, middle panel). This is validated by the analytical gel filtration result on $CstB^{PDO\text{-}RHD}$, indicating the tetrameric status of purified $CstB^{PDO\text{-}RHD}$ (Table 1 and Figure S4E). These findings collectively highlight the substantial differences between the vertebrate core PDOs and bacterial PDO−RHD−Rhod fusion proteins in overall structural organization.

Coupled Persulfide Dioxygenase-Persulfide Transferase (cPDO-PT) Activity of CstB. We employed a fluorescence-based assay to quantify reactant-product profiles obtained with a variety of LMW persulfides as substrates using Fe(II)-loaded wild-type and mutant CstBs to measure the cPDO-PT activity (see Figure 2C, reaction 1). Briefly, reactions were carried out at pH 6.0 for some time t, with the products derivatized with monobromobimane (mBBr), quenched with excess thiol blocker, acidified, filtered, and subjected to C18 reversed-phase HPLC using a methanol-based gradient system at pH 3.9 (Figure 3A).[27,28] The results of a representative assay carried out at high wild-type CstB concentration (400 nM protomer) using bacillithiol persulfide (BSSH) and molecular O_2 to quantify the consumption of substrate and the yield of products are shown (Figure 3A). Two points are apparent from these experiments. First, approximately two mols of BSSH are consumed to yield a single mole equivalent of TS, similar to the finding on CoASSH (Figure 3B). Second, free sulfite is below the level of detection under these conditions (0.62 μM) and thus appears not to be a major product (Figure 3A). This is consistent with tight coupling of the PDO activity and presumed persulfide transferase activity (see Figure 2C, reaction 2; *vide infra*). The latter activity likely employs PDO-catalyzed formation of sulfite or a LMW S-sulfonate to generate TS and a second mole equivalent of RSH, since in stand-alone persulfide dioxygenases, sulfite is the major product.[17]

Utilizing this assay, we next measured the initial rate of TS production as a function of LMW persulfide concentration and saturating O_2 at 40 nM enzyme and obtained Michaelis−

DOI: 10.1021/acs.biochem.5b00584
Biochemistry 2015, 54, 4542−4554

Table 2. Kinetic Characterization of the Coupled Persulfide Dioxygenase-Persulfide Transferase (cPDO-PT) Activity of Wild-Type CstB with Various Substrates[a]

substrate	K_m ($\times 10^{-3}$ M)	V_{max} (μmol TS·min^{-1}·mg^{-1})	k_{cat} (s^{-1})	k_{cat}/K_m ($\times 10^{-3}$ M^{-1}·s^{-1})	specific activity ([substrate] = 1 mM) (μmol TS·min^{-1}·mg^{-1})
CoASSH	1.1 ± 0.3	23.3 ± 2.5	19.3 ± 2.2	17.5 ± 5.1	11.2 ± 1.2
BSSH	1.8 ± 0.4	24.1 ± 3.0	19.7 ± 2.5	10.9 ± 2.8	8.6 ± 1.1
CSSH[b]	20 ± 21	34 ± 32	28 ± 27	1.4 ± 2.0	1.5 ± 0.1
GSSH[b]	7.8 ± 5.0	7.9 ± 4.0	6.5 ± 3.3	0.8 ± 0.7	0.9 ± 0.1

[a]Conditions: 0.04 μM CstB (protomer), 25 mM MES, 100 mM NaBr, pH 6.0, 25 °C. [b]Very low activity (see Figure S6), making it difficult to measure K_m and V_{max} accurately.

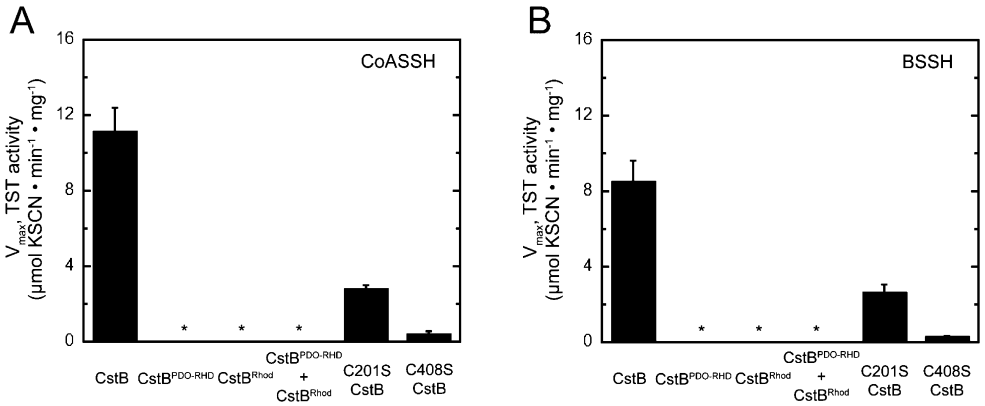

Figure 4. Specific coupled persulfide dioxygenase-persulfide transferase (cPDO-PT) activities of various CstBs determined at 1 mM LMW persulfide substrate: (A) CoASSH and (B) BSSH.

Menten kinetic constants (K_m, V_{max}) for wild-type and mutant CstBs. We find that wild-type CstB preferentially catalyzes the oxidation of CoASSH, with K_m = 1.1 ± 0.3 mM, V_{max} = 23.3 ± 2.5 μmol·min^{-1}·mg^{-1} (Table 2 and Figure 3C), and BSSH, with a K_m = 1.8 ± 0.4 mM, V_{max}= 24.1 ± 3.0 μmol·min^{-1}·mg^{-1} (Table 2 and Figure 3D). In parallel control experiments, CstB does not catalyze the formation of TS from reduced LMW thiol, oxidized LMW disulfide or Na_2S, all used to generate LMW persulfide substrates *in situ* which were used without purification[17] (Figures 3C,D). Cysteine persulfide (CSSH) and glutathione persulfide (GSSH) also serve as persulfide substrates for wild-type CstB but are poorer substrates, with $K_m \geq$ 20 mM for CSSH and K_m = 7.8 ± 5.0 mM for GSSH (Table 2 and Figure S6A,B), the latter of which was reported as major persulfide substrate for human ETHE1. k_{cat}/K_m for these two substrates are only 10−15% that of preferred substrates CoASSH and BSSH (Table 2).

Further investigation of the requirements for cPDO-PT activity reveals that neither isolated CstB$^{PDO-RHD}$ nor CstB^{Rhod} domain is capable of generating TS using CoASSH and BSSH as substrates since no detectable product is observed (Figure 4A,B). Additionally, TS is not observed when the two domains are mixed together and tested in *trans*, a result perhaps attributed to the poor folding of the isolated Rhod domain (*vide supra*). This finding was validated in time-course experiments with CSSH and GSSH serving as persulfide substrates using higher enzyme concentrations due to the low specific activities with CSSH and GSSH (Figure S7A,B). We also tested the activity of C201S and C408S mutant CstBs. C201S displays a specific activity at 1 mM persulfide substrate (≈K_m) that is ≈25% that of wild-type CstB (Figure 4A,B), with the same K_m of 1.1 ± 0.1 mM but a reduced V_{max} of 6.0 ± 0.3 μmol·min^{-1}·mg^{-1} for CoASSH. The C408S enzyme is even less active, with a K_m again comparable to that of wild-type and C201S CstBs, 1.2 ± 0.9 mM, but a substantially reduced V_{max} of 1.0 ± 0.3 μmol·min^{-1}·mg^{-1} using CoASSH as substrate (Figure 4A). Similar findings characterize the reaction for C201S and C408S mutant CstBs with BSSH as substrate (Figure 4B). Further investigation also validates the time-course experiments for C201S and C408S mutant CstBs with CSSH and GSSH serving as persulfide substrates using higher enzyme concentrations (Figure S7C,D). There is no detectable sulfite generated in these assays with mutant CstBs, again consistent with a strong coupling of persulfide dioxygenase and persulfide transferase activities. These data taken collectively reveal that both conserved Cys play important roles in cPDO-PT catalytic efficiency, with C408 clearly being more important for formation of TS product (see Discussion).

Growth Phenotypes of Δ*cstB* Strains under Hydrogen Sulfide Stress. We showed in previous work that CstB is required for *Staphylococcus aureus* to recover from hydrogen sulfide stress and that the growth defect of the Δ*cstB* strain can be complemented by ectopic expression of the wild-type allele from an extrachromosomal plasmid (Figure 5A).[15] Since both C201 and C408 play catalytically important roles in the PDO activity of CstB (see Figure 4), we tested the effect of complementation with mutant allelic *cstB*s under NaHS stress (0.2 mM). We find that the growth defect of Δ*cstB* strain under NaHS stress cannot be efficiently complemented by ectopic expression of either the C201S allele or C408S allele (Figure 5B). The same is true for a strain expressing a C20S CstB allele (Figure 5B). Since we were unable to express recombinant C20S CstB in *E. coli*, C20 may play a structural role in the assembly of active CstB; note that this residue is 100% buried in the structure of CstB$^{PDO-RHD}$ (Figure 2A). Thus, all three Cys substitution mutants fail to efficiently rescue a Δ*cstB* strain stressed with exogenous hydrogen sulfide.

DOI: 10.1021/acs.biochem.5b00584
Biochemistry 2015, 54, 4542−4554

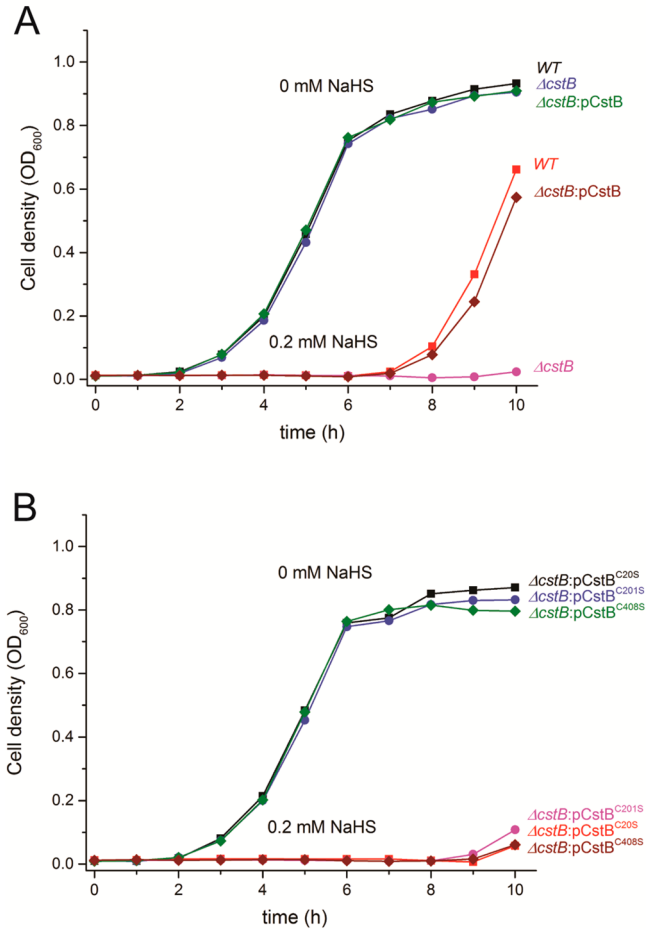

Figure 5. Representative growth curves for wild-type (WT), Δ*cstB*, and plasmid-complemented Δ*cstB* allelic *S. aureus* Newman strains on HHWm media in the presence of 0 and 0.2 mM NaHS added at $t = 0$ h. (A) WT (black square), Δ*cstB* (blue circle), and Δ*cstB*:pCstB (green diamond) strains in the presence of 0 mM NaHS; WT (red square), Δ*cstB* (magenta circle), and Δ*cstB*:pCstB (wine diamond) strains in the presence of 0.2 mM NaHS. Note that both the WT and Δ*cstB*:pCstB strains exhibit a growth lag (≈7 h) in the presence of 0.2 mM NaHS; Δ*cstB* exhibits a more significant growth lag (≈9 h) in the presence of 0.2 mM NaHS. Also note that all strains grow normally in the presence of 0 mM NaHS. (B) Δ*cstB*:pCstB^{C20S} (black square), Δ*cstB*:pCstB^{C201S} (blue circle), and Δ*cstB*: pCstB^{C408S} (green diamond) strains in the presence of 0 mM NaHS; Δ*cstB*:pCstB^{C20S} (red square), Δ*cstB*:pCstB^{C201S} (magenta circle), and Δ*cstB*: pCstB^{C408S} (wine diamond) strains in the presence of 0.2 mM NaHS. Note that all three strains exhibit a more significant growth lag (≈9 h) in the presence of 0.2 mM NaHS. Also note that all strains grow normally in the presence of 0 mM NaHS.

Persulfide Transferase (PT) Activity of CstB. A key aspect of the reactant−product profile obtained as a result of PDO turnover is the consumption of 2 mol equivalents of LMW persulfide and the lack of sulfite as an intermediate product (Figure 3). This leads to the prediction that the C-terminal Rhod domain possesses intrinsic PT activity when provided with sulfite exogenously, independent of Fe(II)-dependent PDO activity (Figure 2C, reactions 1 and 2). It is also known that LMW thiols react noncatalytically to form TS (Figure S8A,B). In order to test this, we measured PT activity in an anaerobic chamber with degassed buffers, using C201S CstB, which has reduced O_2-dependent PDO activity (Figure 4), and relatively low concentrations of each of four LMW persulfide substrates (Figures 6A,B and 9A,B). With correction of the background, non-enzyme-catalyzed rate of TS formation, we find that all three major LMW thiol persulfides from *S. aureus*, including CoASSH, BSSH, and CSSH, can function as the persulfide substrates in this assay with similar catalytic efficiencies, and K_m values are ≈20-fold lower than those found for the preferred substrates for the cPDO-PT activity, CoASSH and BSSH (Table 3). GSSH is also a persulfide substrate for this reaction, but it is characterized by relatively lower substrate affinity and catalytic efficiency (Table 3). As verified above for the cPDO-PT activity, control experiments reveal that C201S CstB does not catalyze any reaction of sulfite with a reduced LMW thiol, oxidized LMW disulfide, or Na_2S to generate TS (Figures 6A,B and S9A,B). In a second control experiment, we show that the double Cys substitution mutant CstB^{2CS} has no PT activity above the background, noncatalyzed rates of TS formation (Figure S8A,B) with any persulfide substrate (Figure S9C−F). These findings collectively suggest that the C-terminal Rhod domain is capable of catalyzing PT activity, and this activity may function in concert with the initial Fe-oxidation step in the PDO activity to generate TS.

Thiosulfate Transferase (TST) Activity of CstB. Free-standing rhodaneses as well as the N-terminal Rhod domain of CstA encoded by the *cst* operon catalyze TS break down to generate a protein persulfide and sulfite.[16,19] When provided with an exogenous nucleophile, e.g., CN^-, the Rhod Cys-derived persulfide turns over to generate thiocyanate anion (SCN^-) and reduced active-site sulfhydryl (Figure 2C, reaction 3). We therefore tested if the wild-type and various mutant forms of CstB possess TST activity and, if so, obtained kinetic parameters under standard assay conditions. Wild-type CstB is characterized by K_m = 1.7 ± 0.2 mM and V_{max} = 10.4 ± 0.6 μmol·min^{-1}·mg^{-1} toward TS in the typical TST assay (Table 4 and Figure 7). Consistent with the prediction of the functional roles of individual domains in CstB, both CstB$^{PDO\text{-}RHD}$ domain and C408S CstB are completely inactive in this assay. In contrast, even though C201S CstB is deficient in cPDO-PT activity, it displays nearly identical kinetic constants as those of wild-type CstB in this assay, with K_m = 2.2 ± 0.4 mM and V_{max} = 11.2 ± 0.9 μmol·min^{-1}·mg^{-1} (Table 4 and Figure 7). As expected, this reveals that the TST activity is contained entirely in the C-terminal Rhod domain of CstB. Interestingly, the isolated CstB^{Rhod} domain is inactive in this TST activity, and mixing stoichiometric CstB^{Rhod} with CstB$^{PDO\text{-}RHD}$ also does not recover activity (Table 4 and Figure 7). One explanation for these findings is that the structure of the isolated CstB^{Rhod} is non-native (Figure S5) and, as a result, the independently purified domains fail to interact productively (Table 4 and Figure 7).

Cellular Thiosulfate Concentrations in Δ*cstB* and Complemented Strains. The experiments described above reveal that CstB catalyzes three distinct reactions *in vitro*, two of which synthesize TS via reduction of LMW persulfides (Figure 2C, reactions 1 and 2) and one of which consumes TS (Figure 2C, reaction 3). We therefore determined the impact of deletion of *cstB* and complementation with wild-type and mutant *cstB* genes on cellular TS concentrations[28] in aerobic mid log *S. aureus* cells as a function of time following induction of the *cst* operon by 0.2 mM NaHS using TS as the sole sulfur source. Previous qRT-PCR experiments revealed that the *cst* operon is maximally induced 10 min following addition of NaHS under these conditions, with mRNA levels returning to near baseline at 30 min.[15]

DOI: 10.1021/acs.biochem.5b00584
Biochemistry 2015, 54, 4542−4554

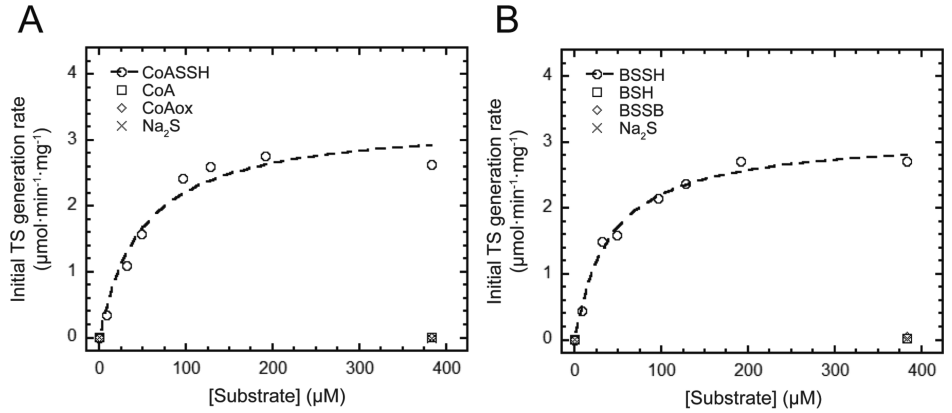

Figure 6. C201S CstB displays persulfide transferase (PT) activity with LMW persulfide substrates. (A) Initial TS generation rates as a function of concentrations of CoASSH (open circles), CoA (open squares), CoAox (open diamonds), and Na_2S (crosses). The dashed, continuous line through the open circles is a fit to the Michaelis–Menten equation, with parameters summarized in Table 3. (B) Initial TS generation rates as a function of concentrations of BSSH (open circles), BSH (open squares), BSSB (open diamonds), and Na_2S (crosses). The dashed, continuous line through the open circles is a fit to the Michaelis–Menten equation, with parameters summarized in Table 3.

Table 3. Comparison of the Kinetic Properties of the Enzyme-Catalyzed Persulfide Transferase (PT) Activity of C201S CstB with Various Substrates[a]

substrate	K_m ($\times 10^{-6}$ M)	V_{max} (μmol TS·min^{-1}·mg^{-1})	k_{cat} (s^{-1})	k_{cat}/K_m ($\times 10^{-3}$ M^{-1}·s^{-1})
CoASSH	49 ± 13	3.3 ± 0.3	2.7 ± 0.2	55.1 ± 15.2
BSSH	40.1 ± 5.2	3.1 ± 0.1	2.5 ± 0.1	62.3 ± 8.4
CSSH	37.0 ± 7.5	2.9 ± 0.2	2.4 ± 0.1	64.8 ± 13.4
GSSH	110 ± 27	4.0 ± 0.4	3.3 ± 0.3	30.0 ± 7.9
KSCN	NA[b]	NA	NA	NA

[a]Conditions: 0.2 μM C201S CstB (protomer), 25 mM MES, 100 mM NaBr, pH 6.0, 25 °C, anaerobic conditions. [b]NA, no observable activity.

Table 4. Comparison of the Thiosulfate Transferase (TST) Activities of Various CstBs[a]

enzyme	K_m ($\times 10^{-3}$ M)	V_{max} (μmol SCN·min^{-1}·mg^{-1})	k_{cat} (s^{-1})	k_{cat}/K_m ($\times 10^{-3}$ M^{-1}·s^{-1})
CstB	1.7 ± 0.2	10.4 ± 0.6	8.5 ± 0.5	5.0 ± 0.7
C201S CstB	2.2 ± 0.4	11.2 ± 0.9	9.2 ± 0.7	4.2 ± 0.8
C408S CstB	NA[b]	NA	NA	NA
$CstB^{PDO\text{-}RHD}$	NA	NA	NA	NA
$CstB^{Rhod}$	NA	NA	NA	NA
$CstB^{PDO\text{-}RHD}$ + $CstB^{Rhod}$	NA	NA	NA	NA

[a]Conditions: 0.4 μM CstB (protomer), 50 mM KCN, 100 mM MES, pH 6.0, 25 °C. [b]NA, no activity observed.

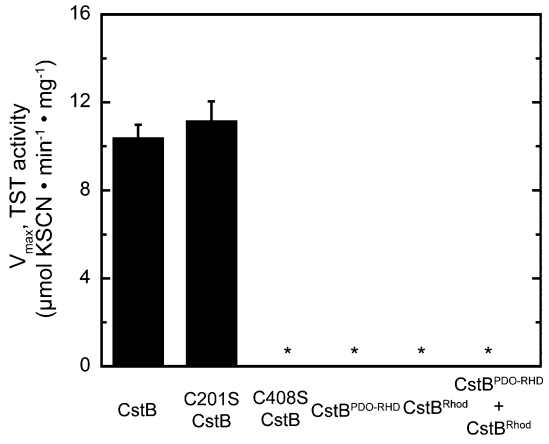

Figure 7. Maximal velocities (V_{max}) for thiosulfate transferase (TST) activities of various CstBs using cyanide anion (CN^-) as sulfane sulfur acceptor. *, none detected (≤0.1 μmol·min^{-1}·mg^{-1} protein). Kinetic constants are summarized in Table 4.

As found previously, TS is below the limit of detection in cells prior to NaHS addition, suggesting that TS is efficiently utilized as the sole sulfur source once it is imported into the cell and that it does not efficiently accumulate.[15] In the wild-type strain, the cellular TS level reaches 15 nmol per mg protein 10 min following NaHS addition and decreases ≈2-fold over the course of 2 h, or approximately two culture doublings (Figure 8). In the Δ*cstB* strain, the cellular TS level is significantly lower at t = 10 min, ≈9 nmol per mg protein, decreasing to ≈6 nmol per mg protein by 2 h. This overall decrease in the cellular TS level in the Δ*cstB* strain can be complemented by extrachromosomal expression of the wild-type *cstB* allele, but it cannot be complemented by the C20S or C201S *cstB* alleles (Figure 8). This suggests that the PDO activity of CstB makes a significant contribution to the cellular TS level under NaHS stress immediately following induction.

In contrast, complementation with the C408S *cstB* allele over-complements the *cstB* deletion, with a wild-type-like cellular TS level observed 10 min postinduction, at ≈15 nmol per mg protein, and remaining elevated throughout the 2 h time course (Figure 8). Since C408 plays roles in all three CstB

DOI: 10.1021/acs.biochem.5b00584
Biochemistry 2015, 54, 4542–4554

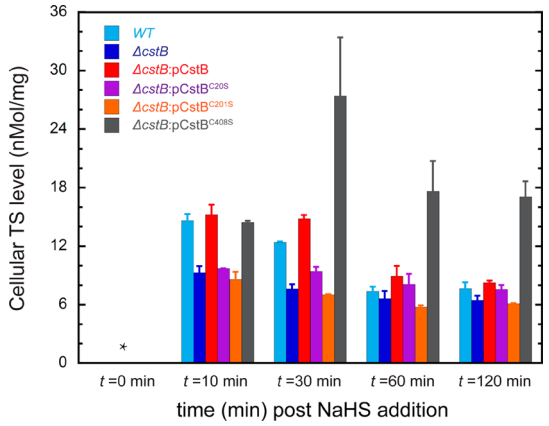

Figure 8. Cellular thiosulfate concentrations in mid log (OD_{600} ≈0.2) wild-type (WT), Δ*cstB*, and plasmid-complemented Δ*cstB* allelic *S. aureus* Newman strains as a function of time following induction of the *cst* operon at *t* = 0 by 0.2 mM NaHS.[15] *, no TS detected (≤0.2 nmol·mg^{-1} protein). The color of the columns is assigned as follows: cyan for WT strain, blue for Δ*cstB* strain, red for Δ*cstB*:pCstB strain, purple for Δ*cstB*:$pCstB^{C20S}$ strain, orange for Δ*cstB*:$pCstB^{C201S}$ strain, and gray for Δ*cstB*:$pCstB^{C408S}$ strain.

activities, but gives rise to a TS level accumulation phenotype opposite to that observed with the C201S mutant, this suggests that the TST activity of the $CstB^{Rhod}$ domain plays a more significant role in governing the cellular TS level following NaHS induction, particularly at longer time points post-induction.

DISCUSSION

In this work, we show that *S. aureus* CstB is a nonheme Fe(II)-containing multidomain persulfide dioxygenase-sulfurtransferase. We describe three separable enzymatic activities of CstB, including an Fe(II)-dependent cPDO-PT activity, the first half of which was previously described for human mitochondrial ETHE1[17] and *Arabidopsis* ETHE1,[22,29] a PT activity, and a TST activity, with the latter two activities catalyzed by the C-terminal Rhod domain (Figure 2C). Thus, CstB possesses two activities that we hypothesize function collaboratively to clear LMW organic persulfides that accumulate in cells when they are exposed to H_2S stress or as a result of misregulation of H_2S homeostasis. The major observable products of the cPDO-PT reaction are TS and reduced LMW thiols, with no detectable sulfite formed as an intermediate (Figure 3A). This finding is in contrast to previous studies of hETHE1 and *Arabidopsis* ETHE1, where sulfite is the only product formed from the oxidation of GSSH; subsequent addition of a classical Rhod domain *in trans* would be anticipated to lead to the formation of TS.[17,29] We show here that the $CstB^{PDO-RHD}$ fragment when mixed with the $CstB^{Rhod}$ does not generate sulfite as product, as could be expected if the two enzyme activities were uncoupled as a result of reconstitution in *trans*. Clearly, C201S CstB has significant PT activity using sulfite as an exogenous nucleophile, thus suggesting that it may not be likely that sulfite is channeled in some way to the C408 active site directly from the Fe active site. How the Fe and C408 active sites communicate with one another is therefore unknown. We do show that the cPDO-PT activity is highest with persulfide substrates derived from major cellular thiols in *S. aureus*, including bacillithiol and coenzyme A, and is less efficient when glutathione and cysteine persulfides are used as substrates (Table 2).

CstB is a homotetramer in solution and is characterized by a core PDO domain that is structurally superimposable on *Arabidopsis* ETHE1-like protein and hETHE1 fused to a middle RHD domain that is packed against the core PDO domain but lacks an active site cysteine (Figure 2B). This RHD may well provide the majority of the interprotomer contacts that stabilize the tetramer in solution as well (Figure S3). In CstB, this PDO−RHD is connected to a C-terminal classical Rhod domain that harbors an active site C408. This latter domain was not resolved in the crystal structure of CstB2, but it is found in a CstB-like protein from *A. acidocaldarius* (Figure 2B). The biochemical activity of this *A. acidocaldarius* CstB-like protein, to our knowledge, is not yet known, so these structural comparisons must be taken with a degree of caution. Nonetheless, it is striking that all three Cys in *S. aureus* CstB are conserved in this CstB-like protein, including the equivalent of C201, which makes close approach to an active site metal ion and itself is coordinated in exactly the same way as in CstB, hETHE1, and the *Arabidopsis* ETHE1-like protein. If this *A. acidocaldarius* CstB-like protein is a good structural model of CstB, then this reveals that C408 and the open coordination site of the Fe atom are indeed oriented toward one another within the same subunit, but they may be too far apart in this conformation to drive a concerted oxidation of the terminal persulfide sulfur atom at the Fe active site to TS without release of sulfite. Other plausible scenarios include a Rhod domain of one subunit making closer approach to the PDO domain Fe(II) atom of an adjacent subunit or that the flexible loop containing C201 facilitates intramolecular transfer from the PDO active site to C408.

Interestingly, wild-type and C201S CstBs have identical TST activities and, in fact, exhibit kinetic parameters that are very similar to those measured for the N-terminal Rhod domain of *S. aureus* CstA (Table 4).[16] This suggests that the access of $CstB^{Rhod}$ to TS substrate is not rate limiting even in the context of intact CstB, thus providing another argument against a close structural approach of the Fe(II) and C408 active sites. In fact, it is this TST activity that may dominate cellular TS metabolism following acute-phase NaHS stress (Figure 8). CstA is also under the transcriptional control of the persulfide sensor CstR,[15] and genes encoding CstA and CstB may comprise a minimal LMW persulfide clearance system that is duplicated in many methicillin-resistant strains (Figure S1), either via reduction of RSSH to RSH concomitant with the generation of TS via CstB or, as in the case of CstA, by reacting directly with LMW persulfides and inorganic polysulfides to generate CstA-bound persulfides as a means to assimilate sulfide-derived sulfur.[16] In preliminary experiments, we have tested if a CstA-bound persulfide can function as a substrate (at 200 μM) for the cPDO-PT activity of CstB and were unable to measure activity (J. Shen and H. Peng, unpublished results). Since the multidomain sulfurtransferase CstA is capable of shuttling persulfides between the N-terminal Rhod and middle TusA domain,[16] the lifetime of a persulfide on the Rhod domain may be short; furthermore, we have not yet tested if the C-terminal TusD domain is part of this CstA persulfide shuttle or is capable of functioning as a direct persulfide donor to CstB. Alternatively, the TS generated by the cPDO-PT activity of CstB is shuttled directly to CstA to generate mobilizable sulfur in the form of protein-bound persulfides (Figure 9). Finally, it also seems possible, by analogy with the mitochondrial sulfide oxidation system, that an SQR-bound persulfide might function

DOI: 10.1021/acs.biochem.5b00584
Biochemistry 2015, 54, 4542−4554

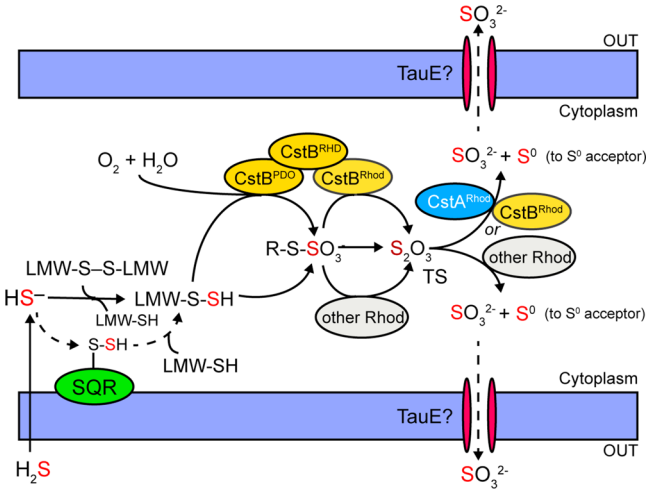

Figure 9. Current model for cellular H_2S detoxification in *Staphylococcus aureus* highlighting the known or proposed enzymatic activities encoded by the *cst* operon (this work). Extracellular H_2S freely penetrates the cell membrane and exists as HS^- once in the cytoplasm. SQR then carries out the initial two-electron oxidation of HS^- to form SQR-bound persulfide, and the SQR-bound persulfide is transferred to reduced cellular LMW thiols (LMW-SH) to form LMW persulfides (LMW-SSH), which can also be generated from HS^- directly via reaction with oxidized LMW thiols (LMW-S-S-LMW). In the presence of molecular oxygen (O_2), CstB^{PDO} further oxidizes LMW persulfides to possibly form a LMW thiol-S-sulfonate or CstB-S-sulfonate (denoted R-S-SO_3^-) intermediate, which requires further investigation. Free thiosulfate (TS) is then immediately generated either through the persulfide transferase activity of CstB^{Rhod} or other cellular rhodanese proteins (other Rhod) or directly generated via reaction of a LMW persulfide with LMW thiol-S-sulfonate or CstB-S-sulfonate. Finally, accumulating thiosulfate is processed by the thiosulfate sulfurtransferase activities of CstB^{Rhod}, CstA^{Rhod}, or other cellular rhodanese proteins. Sulfite (SO_3^{2-}) is effluxed from the cell (perhaps by TauE), and sulfane sulfur (S^0) is proposed to be transferred to as yet unknown downstream cellular sulfur acceptor(s) for assimilation.

as a persulfide donor for CstB.[30] Preliminary experiments to distinguish among these possibilities are in progress.

The chemical mechanism of the PDO activity is unknown, as is the functional role of the conserved C201. Reduced Fe(II) is required for activity and, by analogy to cysteine dioxygenase (CDO), may involve direct coordination of the persulfide substrate via one or both sulfur atoms to the side of the Fe(II) that is free of protein-derived ligands (Figure 2B).[31] By further analogy to CDO, a high-valent Fe-oxo species is the likely oxidant, which leads to the formation of a Fe-bound organic LMW-S-sulfinate, $RSSO_2$, followed by addition of H_2O to generate $RSSO_3$. Then, in the second phase of the reaction, the S−S bond may be cleaved by an attacking LMW persulfide or a Rhod-bound persulfide formed as a result of the PT activity of CstB to generate TS and a second equivalent of LMW thiol. C201 could function in this second step by forming an enzyme-bound S-sulfocysteine intermediate, which is then attacked by the C408 persulfide. The low, but detectable, level of cPDO-PT activity of C408S CstB (Figure 4) may derive from LMW persulfides reacting with LMW thiol-S-sulfonate or CstB-S-sulfonate, potentially generated by the PDO activity of C408S CstB. Additional experiments are required to substantiate this mechanistic model, including efforts to trap a possible enzyme-bound covalent intermediate in this process. It is unknown, for example, if there are two physically distinct RSSH binding sites, one for the initial oxidation and another for the persulfide transfer step.

We note that candidate CstR-regulated genes near a clearly identifiable, consensus *cst* operator sequence[14] are also found in two other Gram-positive human pathogens, *Enterococcus facaelis* and *Bacillus anthracis*. In both instances, downstream genes include two stand-alone candidate Rhod homology domains that flank a gene that is annotated as a CoA disulfide reductase-rhodanese homology domain protein (CoADR-RHD). In both organisms, an authentic CoADR is encoded elsewhere in the genome,[32] suggesting an alternate function for CoADR-RHD. Interestingly, the crystal structure of *B. anthracis* CoADR-RHD has been solved, and biochemical experiments carried out prior to the knowledge of CstR-regulated cellular persulfide chemistry[15] reveal that the substrate binding channel for CoA is unlikely to accommodate the CoA disulfide. Furthermore, the two cysteines, one each in the core CoADR and rhodanese domains on a complementary subunit, although separated by ≈25 Å, are proposed to communicate with one another via the long swinging pantethiene arm.[33] We speculate that both *B. anthracis* and *E. facaelis* CoADR-RHDs have evolved to catalyze the reduction of CoASSH formed under conditions of sulfide or RSS stress to the free thiol concomitant with the generation of a RHD enzyme-bound persulfide, which may then be assimilated by cellular components in some way via a subsequent persulfide transfer. Thus, CstB and CoADR-RHD may provide distinct solutions to a common problem, i.e., to clear CoASSH (CoA is a major cellular thiol in both *S. aureus*[32] and *B. anthracis*) that may accumulate under conditions of H_2S toxicity. It will be of interest, for example, to determine if CoADR-RHD can functionally complement a Δ*cstB S. aureus* Newman strain. Finally, the function of the *cst* operon in general microbial physiology is not yet firmly established, but at least one transcriptomic experiment in *S. aureus* strain N315 ties strong induction of the *cst* operon-encoded genes, including *cstB*, to nitric oxide-mediated dispersal of staphylococcal biofilms.[34] Efforts are underway to link this process with the need to regulate endogenous hydrogen sulfide levels in this human pathogen.

■ ASSOCIATED CONTENT

Supporting Information

NMR spectroscopy methods. Figure S1: Chromosomal gene arrangement of *cst* and *cst*-like operons in various strains of *Staphylococcus aureus* reveals that *cst*-like operons are frequently associated with methicillin-resistance genes. Figure S2: Structure-based sequence alignment of CstB with other persulfide dioxygenases. Figure S3: CstB2 crystal structure asymmetric unit suggests likely tetramer interfaces. Figure S4: Gel filtration profiles for wild-type CstB, missense mutant CstBs, and domain fragments of CstB. Figure S5: Sub-region of the $^1H-^1H$ NOESY spectrum of CstB^{Rhod} highlighting amide-aliphatic NOEs. Figure S6: Coupled persulfide dioxygenase-persulfide transferase (cPDO-PT) activity of CstB with alternative persulfide substrates. Figure S7: Coupled persulfide dioxygenase-persulfide transferase (cPDO-PT) activities for wild-type CstB, domain fragments of CstB, and missense mutant CstBs with alternative persulfide substrates. Figure S8: Representative time-course kinetics indicating LMW persulfide substrates react with sulfite to generate TS noncatalytically. Figure S9: C201S CstB displays persulfide transferase (PT) activity with other LMW persulfide substrates, and CstB^{2CS}

DOI: 10.1021/acs.biochem.5b00584
Biochemistry 2015, 54, 4542−4554

displays no significant activity with any LMW persulfide substrate tested. The Supporting Information is available free of charge on the ACS Publications website at DOI: 10.1021/acs.biochem.5b00584.

AUTHOR INFORMATION

Corresponding Author

*Tel: 812-856-3178; Fax: 812-856-5710; E-mail: giedroc@indiana.edu.

Present Address

#Department of Chemistry, Salve Regina University, Newport, Rhode Island 02840 United States

Author Contributions

J.S. and D.P.G. designed the research; J.S. performed the research; M.E.K. and R.N.A. provided reduced and oxidized bacillithiol; K.A.H. helped J.S. perform EPR experiments, with the data being analyzed by K.A.H.; K.A.E. performed the bioinformatics and structural analysis of CstB and *cst* operon synteny; and J.S. and D.P.G. wrote the manuscript.

Funding

The authors gratefully acknowledge support by the NIH (R01 GM097225 to D.P.G., R01 GM030910 to R.N.A., and T32 ES007028 to M.E.K.).

Notes

The authors declare no competing financial interest.

⊥R.N.A. is deceased.

ACKNOWLEDGMENTS

This work will be submitted by J.S. to the Graduate School of Indiana University in partial fulfillment of the requirements for the Ph.D. in Biochemistry. The authors wish to thank Jay Levy for help in setting up the HPLC used for sulfur metabolite analyses. We also thank Drs. Hongwei Wu, Joey Braymer, and Justin Luebke for many helpful discussions on this project. The NMR instrumentation at Indiana University was generously supported by the Indiana METACyt Initiative, funded in part through a major grant from the Lilly Endowment, Inc.

DEDICATION

The authors wish to dedicate this manuscript to the memory of Prof. Richard N. Armstrong.

ABBREVIATIONS

Cst, CsoR-like sulfurtransferase; PDO, persulfide dioxygenase; PT, persulfide transferase; RHD, rhodanese homology domain; Rhod, rhodanese; TS, thiosulfate; TST, thiosulfate sulfurtransferase

REFERENCES

(1) Mathai, J. C., Missner, A., Kugler, P., Saparov, S. M., Zeidel, M. L., Lee, J. K., and Pohl, P. (2009) No facilitator required for membrane transport of hydrogen sulfide. *Proc. Natl. Acad. Sci. U. S. A. 106*, 16633−16638.

(2) Cooper, C. E., and Brown, G. C. (2008) The inhibition of mitochondrial cytochrome oxidase by the gases carbon monoxide, nitric oxide, hydrogen cyanide and hydrogen sulfide: chemical mechanism and physiological significance. *J. Bioenerg. Biomembr. 40*, 533−539.

(3) Dorman, D. C., Moulin, F. J., McManus, B. E., Mahle, K. C., James, R. A., and Struve, M. F. (2002) Cytochrome oxidase inhibition induced by acute hydrogen sulfide inhalation: correlation with tissue sulfide concentrations in the rat brain, liver, lung, and nasal epithelium. *Toxicol. Sci. 65*, 18−25.

(4) Truong, D. H., Eghbal, M. A., Hindmarsh, W., Roth, S. H., and O'Brien, P. J. (2006) Molecular mechanisms of hydrogen sulfide toxicity. *Drug Metab. Rev. 38*, 733−744.

(5) Lin, V. S., Chen, W., Xian, M., and Chang, C. J. (2014) Chemical probes for molecular imaging and detection of hydrogen sulfide and reactive sulfur species in biological systems. *Chem. Soc. Rev. 44*, 4596−4618.

(6) Ida, T., Sawa, T., Ihara, H., Tsuchiya, Y., Watanabe, Y., Kumagai, Y., Suematsu, M., Motohashi, H., Fujii, S., Matsunaga, T., Yamamoto, M., Ono, K., Devarie-Baez, N. O., Xian, M., Fukuto, J. M., and Akaike, T. (2014) Reactive cysteine persulfides and S-polythiolation regulate oxidative stress and redox signaling. *Proc. Natl. Acad. Sci. U. S. A. 111*, 7606−7611.

(7) Kabil, O., and Banerjee, R. (2010) Redox biochemistry of hydrogen sulfide. *J. Biol. Chem. 285*, 21903−21907.

(8) Kolluru, G. K., Shen, X., Bir, S. C., and Kevil, C. G. (2013) Hydrogen sulfide chemical biology: pathophysiological roles and detection. *Nitric Oxide 35*, 5−20.

(9) Paul, B. D., and Snyder, S. H. (2012) H(2)S signalling through protein sulfhydration and beyond. *Nat. Rev. Mol. Cell Biol. 13*, 499−507.

(10) Shatalin, K., Shatalina, E., Mironov, A., and Nudler, E. (2011) H_2S: a universal defense against antibiotics in bacteria. *Science 334*, 986−990.

(11) Tiranti, V., Viscomi, C., Hildebrandt, T., Di Meo, I., Mineri, R., Tiveron, C., Levitt, M. D., Prelle, A., Fagiolari, G., Rimoldi, M., and Zeviani, M. (2009) Loss of ETHE1, a mitochondrial dioxygenase, causes fatal sulfide toxicity in ethylmalonic encephalopathy. *Nat. Med. 15*, 200−205.

(12) Czyzewski, B. K., and Wang, D. N. (2012) Identification and characterization of a bacterial hydrosulphide ion channel. *Nature 483*, 494−497.

(13) Kluytmans, J., van Belkum, A., and Verbrugh, H. (1997) Nasal carriage of *Staphylococcus aureus:* epidemiology, underlying mechanisms, and associated risks. *Clin. Microbiol. Rev. 10*, 505−520.

(14) Grossoehme, N., Kehl-Fie, T. E., Ma, Z., Adams, K. W., Cowart, D. M., Scott, R. A., Skaar, E. P., and Giedroc, D. P. (2011) Control of copper resistance and inorganic sulfur metabolism by paralogous regulators in *Staphylococcus aureus*. *J. Biol. Chem. 286*, 13522−13531.

(15) Luebke, J. L., Shen, J., Bruce, K. E., Kehl-Fie, T. E., Peng, H., Skaar, E. P., and Giedroc, D. P. (2014) The CsoR-like sulfurtransferase repressor (CstR) is a persulfide sensor in *Staphylococcus aureus*. *Mol. Microbiol. 94*, 1343−1360.

(16) Higgins, K. A., Peng, H., Luebke, J. L., Chang, F. M., and Giedroc, D. P. (2015) Conformational analysis and chemical reactivity of the multidomain sulfurtransferase, *Staphylococcus aureus* CstA. *Biochemistry 54*, 2385−2398.

(17) Kabil, O., and Banerjee, R. (2012) Characterization of patient mutations in human persulfide dioxygenase (ETHE1) involved in H_2S catabolism. *J. Biol. Chem. 287*, 44561−44567.

(18) Gunnison, A. F. (1981) Sulphite toxicity: a critical review of in vitro and in vivo data. *Food Cosmet. Toxicol. 19*, 667−682.

(19) Cipollone, R., Ascenzi, P., and Visca, P. (2007) Common themes and variations in the rhodanese superfamily. *IUBMB Life 59*, 51−59.

(20) Weinitschke, S., Denger, K., Cook, A. M., and Smits, T. H. (2007) The DUF81 protein TauE in Cupriavidus necator H16, a sulfite exporter in the metabolism of C2 sulfonates. *Microbiology 153*, 3055−3060.

(21) McCoy, J. G., Bingman, C. A., Bitto, E., Holdorf, M. M., Makaroff, C. A., and Phillips, G. N., Jr. (2006) Structure of an ETHE1-like protein from *Arabidopsis thaliana*. *Acta Crystallogr., Sect. D: Biol. Crystallogr. 62*, 964−970.

(22) Holdorf, M. M., Owen, H. A., Lieber, S. R., Yuan, L., Adams, N., Dabney-Smith, C., and Makaroff, C. A. (2012) *Arabidopsis* ETHE1 encodes a sulfur dioxygenase that is essential for embryo and endosperm development. *Plant Physiol. 160*, 226−236.

(23) Pettinati, I., Brem, J., McDonough, M. A., and Schofield, C. J. (2015) Crystal structure of human persulfide dioxygenase: structural

DOI: 10.1021/acs.biochem.5b00584
Biochemistry 2015, 54, 4542−4554

basis of ethylmalonic encephalopathy. *Hum. Mol. Genet. 24*, 2458−2469.
(24) Holdorf, M. M., Bennett, B., Crowder, M. W., and Makaroff, C. A. (2008) Spectroscopic studies on *Arabidopsis* ETHE1, a glyoxalase II-like protein. *J. Inorg. Biochem. 102*, 1825−1830.
(25) Lamers, A. P., Keithly, M. E., Kim, K., Cook, P. D., Stec, D. F., Hines, K. M., Sulikowski, G. A., and Armstrong, R. N. (2012) Synthesis of bacillithiol and the catalytic selectivity of FosB-type fosfomycin resistance proteins. *Org. Lett. 14*, 5207−5209.
(26) Ellman, G. L. (1959) Tissue sulfhydryl groups. *Arch. Biochem. Biophys. 82*, 70−77.
(27) Newton, G. L., Dorian, R., and Fahey, R. C. (1981) Analysis of biological thiols: derivatization with monobromobimane and separation by reverse-phase high-performance liquid chromatography. *Anal. Biochem. 114*, 383−387.
(28) Newton, G. L., Arnold, K., Price, M. S., Sherrill, C., Delcardayre, S. B., Aharonowitz, Y., Cohen, G., Davies, J., Fahey, R. C., and Davis, C. (1996) Distribution of thiols in microorganisms: mycothiol is a major thiol in most actinomycetes. *J. Bacteriol. 178*, 1990−1995.
(29) Krussel, L., Junemann, J., Wirtz, M., Birke, H., Thornton, J. D., Browning, L. W., Poschet, G., Hell, R., Balk, J., Braun, H. P., and Hildebrandt, T. M. (2014) The mitochondrial sulfur dioxygenase ethylmalonic encephalopathy protein1 is required for amino acid catabolism during carbohydrate starvation and embryo development in *Arabidopsis*. *Plant Physiol. 165*, 92−104.
(30) Kabil, O., Motl, N., and Banerjee, R. (2014) HS and its role in redox signaling. *Biochim. Biophys. Acta, Proteins Proteomics 1844*, 1355−1366.
(31) Joseph, C. A., and Maroney, M. J. (2007) Cysteine dioxygenase: structure and mechanism. *Chem. Commun.*, 3338−3349.
(32) delCardayre, S. B., Stock, K. P., Newton, G. L., Fahey, R. C., and Davies, J. E. (1998) Coenzyme A disulfide reductase, the primary low molecular weight disulfide reductase from *Staphylococcus aureus*. Purification and characterization of the native enzyme. *J. Biol. Chem. 273*, 5744−5751.
(33) Wallen, J. R., Mallett, T. C., Boles, W., Parsonage, D., Furdui, C. M., Karplus, P. A., and Claiborne, A. (2009) Crystal structure and catalytic properties of *Bacillus anthracis* CoADR-RHD: implications for flavin-linked sulfur trafficking. *Biochemistry 48*, 9650−9667.
(34) Schlag, S., Nerz, C., Birkenstock, T. A., Altenberend, F., and Gotz, F. (2007) Inhibition of staphylococcal biofilm formation by nitrite. *J. Bacteriol. 189*, 7911−7919.

DOI: 10.1021/acs.biochem.5b00584
Biochemistry 2015, 54, 4542−4554